



# Polymeric ion exchanger supported ferric oxide nanoparticles as adsorbents for toxic metal ions from aqueous solutions and acid mine drainage

Caroline Lomalungelo Dlamini<sup>1</sup> · Lueta-Ann De Kock<sup>1</sup> · Kebede Keterew Kefeni<sup>1</sup> · Bhekis Brilliance Mamba<sup>1</sup> · Titus Alfred Makudali Msagati<sup>1</sup>

Received: 6 May 2018 / Accepted: 25 June 2019 / Published online: 1 July 2019  
© Springer Nature Switzerland AG 2019

## Abstract

**Background** Acid mine drainage (AMD) is a worldwide industrial pollution of grave concern. AMD pollutes both water sources and the environment at large with dissolved toxic metals which are detrimental to human health. This paper reports on the preparation of polymeric ion exchange resins decorated with hydrated iron oxides and their application for the ecological removal of toxic metals ions from AMD.

**Methods** The hydrated iron oxide particles were incorporated within commercial chelating ion exchange resins using the precipitation method. The synthesised hybrid resins were then characterized using appropriate spectroscopic and solid-state techniques. The metal ion levels were measured using the inductively coupled plasma-optical emission spectrometer (ICP-OES). The optimization of contact time, pH, and adsorbent dosage were conducted to enhance the efficiency of adsorption of toxic metals onto the hybrid organic/inorganic nanosorbents. Kinetics and adsorption isotherms were constructed to study the adsorption mechanisms of the adsorbents.

**Results** The results showed that the dispersed Fe-O is hydrated and amorphous within the hybrid materials. The adsorption kinetics followed the pseudo-second-order shown by the high  $R^2$  values. The hybrid adsorbents were finally tested on environmental AMD samples and were able to remove toxic metals Al, Cd, Co, Cr, Cu, Fe, Mn, Ni, Pb and Zn at various removal degrees.

**Conclusion** Solution pH played a crucial role in the adsorption of toxic metals on hybrid iron oxide adsorbents. The hybrid TP-260 HFO had higher affinity for toxic metals than other prepared adsorbents thus has a potential for acidic mine water pollution remediation. The adsorbed Al(III) can be recovered using NaCl-NaOH binary solution from the loaded resins.

**Keywords** Acid mine water · Adsorption · Hybrid chelating resin · Hydrated iron oxide · Toxic metal

## Introduction

Minerals and metal extraction is one of the most vital economic activities to many of the developing economies. In the mining industry, minerals of interest, such as gold, usually occur together with various metal sulphides, of which sulphides pyrite, (iron sulphide), is of grave concern because upon

exposure to air and water it produces an acidic effluent known as acid mine drainage (AMD) [1]. Once AMD is formed it renders the water acidic, thus affecting aquatic organisms and pollutes the whole environment. Acidic water pollutes the environment by leaching out an array of toxic metals from every environmental compartment that comes in contact with making mine water heavily laden with dissolved toxic metals that bears grievous human health and ecological risks [2, 3]. These toxic metals, are known to be bioaccumulative systemic toxins even at trace levels, and can significantly impair the environment. Therefore, it is imperative to remove these dissolved metals from acid mine water to save the environment.

According to the literature, the majority of the traditional methods for the removal of toxic metals from water make use of chemicals. These methods include neutralization using

✉ Titus Alfred Makudali Msagati  
msagatam@unisa.ac.za

<sup>1</sup> College of Science Engineering and Technology, Nanotechnology and Water Sustainability Research Unit, University of South Africa, The Science Campus, P/Bag X6 Roodepoort, Johannesburg 1709, South Africa

industrial by-products and ion-exchange [4, 5]. Active technologies including the high density sludge (HDS) process which involve neutralization of AMD using lime and limestone followed by aeration, using pure oxygen or air, to oxidize ferrous iron to ferric iron [6]. However, this process discharges the toxic metals which were in the AMD as hydroxides, including radionuclides, back into the environment. Another process, the alkali-barium-calcium (CSIR ABC) is used principally for the removal of sulphates by chemical precipitation though it has the potential to remove metals from AMD as well [1]. This process integrates neutralization using lime/limestone with precipitation of sulphates using barium carbonate. The limitation of the CSIR ABC is that it is associated with the production of toxic barium ion by-products and discharges them into the environment. Another process that has been used is the SAVMIN process which involve three sequential treatment steps: neutralisation that results in the removal of metals and gypsum crystallisation, followed by selective sulphate removal by ettringite precipitation and lastly is the softening and pH adjustment by re-carbonation which includes aluminium recovery [6]. However, these chemicals turn to be another environmental hazard in the sense that they create secondary pollution and they also exhibit poor compatibility with biological processes in the environment [7]. Therefore, green and sustainable technologies for the removal of toxic metals from acidic water are being sought worldwide [8]. This is one of the sound actions to be taken in order to address the environmental pollution challenges adequately and appropriately. One of the most appropriate and attractive remediation technology involve the use of adsorption processes. Adsorption may be preferred as an alternative technology because, besides being efficient and economic, the metals adsorbed from onto the adsorbent can be desorbed and recovered for economic purposes [9]. In addition, adsorption is an environmentally, ecologically and economically sound technology for the remediation of toxic metal pollution in the aquatic environment. This method drives towards a zero-waste as well as near zero-cost technology, which is most desirable. Another advantage of adsorption processes is that, the technology is cost effective partly due to the fact that, the adsorbent can be regenerated and be re-used repeatedly without affecting the performance significantly [9, 10].

Literature reports suggest that, numerous inorganic adsorbent materials have been developed using nano-sized metal oxides as part of the composites [11]. The metal oxide nanoparticles (MONPs) are preferred adsorbents because they exhibit high adsorption capacity that can be achieved in a very short time [12, 13]. Moreover, in most cases, the metal oxide nanoparticles' surfaces are amphoteric implying that they can either donate or accept electrons depending on the pH of the surrounding solution or matrix. Below their iso-electric point ( $\text{pH}_{\text{pzc}}$ ), the metal oxide accepts electrons acting as a Lewis acid while above this point, they donate the electrons adopting

a Lewis base behaviour [14]. Not only that, synthesis of these nanoparticles is safe, simple and cost effective.

Of the MONPs, hydrated iron oxide (HFO) is the most widely used because it is environmentally benign, cost effective, readily available and chemically stable over a wide range of pH [15, 16]. Nassar [17] reviewed the use of iron oxide NPs for the removal of different pollutants from wastewater. and concluded that iron oxide NPs can be used as an effective technology to treat complex wastewaters and the spent NPs can be regenerated by altering the pH. Klimkova et al. [18] used zero valent iron NPs, which are hydrated in solution, to remove toxic metals from AMD and from the study it was found that the hydrated iron NPs were able to appreciably reduce Cr, Cu, Ni, As, Be, Cd, U, V and Zn levels in the acidic water. However, in as much as metal oxide NPs are good adsorbents for the removal of toxic metals from solution, they suffer from aggregation problems which cause the nanoparticles to lose their nano-dimensions hence adversely affecting their efficient performance. Not only that, NPs also lack the mechanical strength and stability to be used in fixed-bed reactors for practical application [12, 15, 19]. Moreover, excessive pressure drops and poor durability due to the small size of the NPs render them unsuitable for use in large scale water treatment [16, 20, 21]. To overcome these challenges nanoparticles are usually embedded into polymeric (organic) material for support. Ion exchange resins are a good host material for the metal oxide nanoparticles as suggested by Cumbal et al. [19].

Ion exchange resins embedded metal or metal oxide nanoparticles are smart materials with excellent selectivity and high adsorption capacity of the removal of toxic metals from solutions [13]. The enhanced adsorption performance is attributed to the characteristics of both the host resin and the immobilised metal oxide nanoparticles. The non-diffusible charges on the functional groups of the ion exchange host resin allow counterions into the beads and reject co-ions, a phenomenon known as Donnan membrane effect [16]. The Donnan effect enables the adsorbent to be highly selective depending on their functional group fixed charge i.e. negative fixed charges will allow only cations in and likewise positive fixed charges will allow only anions in. On the other hand, the dispersed MONPs can adsorb both cations and/or anions depending on the pH of the surrounding solution, as mentioned earlier, and what has been selected in by the host material. Transition metal ions, which are usually divalent, are preferred by the MO adsorbents over common ions, the monovalent alkaline and divalent alkaline-earth metal ions [14]. This choice is attributed to the fact that transition metal ions have an empty d-orbital which enables them to form coordinate bonds with the MO adsorbents. Hence, hybrid ion exchange metal oxide (HIXMO) nanocomposites are excellent adsorbents that can adsorb toxic metals ions from highly acidic solutions, and they are therefore a good candidate for the

removal of toxic metals from acid mine drainage polluted waters.

Many reports have published work that involves incorporating Fe oxide NPs into both natural and synthetic ion-exchange resins forming hybrid ion exchangers that retain the adsorptive properties of the metal oxide nanoparticles [14, 16, 20, 22]. The resin in the nanocomposite also retains its properties as well as providing the mechanical strength lacked by the NPs. Doula [23] used a natural zeolite, clinoptilolite, as a cation exchanger support for Fe oxide NPs to concurrently remove Cu, Zn and Mn from water. The result obtained showed that the natural hybrid has high adsorption capacity of the heavy metals yielding water suitable for domestic purposes. Hybrids of Fe (III) oxide NPs dispersed within a synthetic cation exchange resin (HCIX) have been prepared [16, 20]. Cumbal and SenGupta [16] reported the adsorption of perchlorate and arsenic from water using a hybrid iron oxide nanoparticle anion exchange resin (HAIX) and HCIX. They found that HAIX removed both anions while HCIX was unable to remove them due to the Donnan membrane effect. Sarkar et al. [12] conducted a pilot scale experiment on the use of a commercial Fe hybrid anionic exchange resin, for the removal of As from water in the presence of competing ions. The study found that the commercial Fe hybrid exceeded other Fe oxide based nanosorbents in terms of their performance. The use of Fe hybrid anion exchange resin for the selective removal of other anionic ligand pollutants like  $\text{HPO}_4^{2-}$  from water has also been reported by several researchers [14, 22].

Most of the studies are based on cation and anion exchange resins as host materials for the HFO NPs; hybrid cation exchange resins for the removal of metal ions while hybrid anion exchange resins have been used for the removal of anionic ligands from solutions. Some studies have proved that chelating resins have superior performances over both cationic and anionic resins [24] yet there is very little literature available on their use as host material for metal oxide particles. Donia et al. [25] used an amine and thiol functionalized chelating resin embedded with magnetite ( $\text{F}_3\text{O}_4$ ) to remove Ag (I) from solution at neutral pH. It was found that the metal ions have a strong affinity for the thiol groups resulting in 90% removal from solution. Donia et al. [26] also dispersed  $\text{F}_3\text{O}_4$  particles into a modified chitosan chelating resin and used it to successfully remove Au (III) from a highly acidic solution (pH 0.5) and Ag (I) at neutral pH.

So far, hybrid iron oxide embedded chelating resins have only been used for valuable metal recovery from solutions. Therefore this present work is aimed at providing an insight on the use of hybrid iron oxide adsorbent based on chelating resins as the host material for the removal of toxic metals from acidic water. The objective of this study is, firstly, to synthesize a variety of hybrid iron oxide nanocomposites using macroporous chelating resins with different functional groups

as the host material for HFO nanoparticles. Secondly, to establish the sorption properties of these hybrid materials on Al in the presence of Mn in highly acidic sulphate laden synthetic water. Lastly, to remove toxic metals from real AMD using these adsorbents.

## Experimental

### Synthesis of hybrid Fe-O adsorbents

All chemicals used in this work were of analytical grade purchased from Sigma-Aldrich (Johannesburg, South Africa). Five different macroporous polystyrene cross-linked with divinyl benzene (DVB) resins were used as host materials for the hybrid Fe-O adsorbents to compare the effects of various functional groups on the toxic metal adsorption potential. Three of these host resins (TP-260, TP-207 and TP-214) were of the weakly acidic chelating type while the other two (M4195 and IRA-900), were anionic - weakly basic chelating and a strongly basic anion exchangers, respectively. The host resins were washed by shaking 50 g of each in 250 mL DI water in a pre-washed conical flask for 2 hours using an orbital shaker set at a speed of 150 rpm. This procedure was carried out 3 times with fresh DI water each time. A 1 M ammonium ferric sulphate dodecahydrate solution was prepared using deionized water and used to load the Fe (III) ions into the TP-260 host resin. All the other host resins were loaded using 1M ferric chlorid solution. Metal loading solutions for anion exchangers were prepared by dissolving the metal salt in 1 M dilute HCl in an ice bath [15]. The full synthesis procedure was done in three steps. The first step was the loading of the iron into the 50 g washed resin by shaking with 250 mL loading solution in an orbital shaker set at 150 rpm in room temperature for 24 hours. The supernatant was decanted and discarded appropriately. The next step was the simultaneous desorption and precipitation of the ferric ions loaded into the resins by shaking with 250 mL of 1 M each of a binary NaCl-NaOH solution under the same conditions as in the previous step. The solution was decanted and discarded likewise and the resin beads were then washed with DI water several times to remove all residual binary solution. The clean resins were finally dried in an oven set at 40 °C overnight for 16 hours and the was ready for use. .

### Characterization of synthesized resins

Physical characterization was carried out on both the host and hybrid resins. The crystallinity of the synthesized composites was investigated using XRD, model Rigaku Smartlab X-ray Diffractometer. The morphology as well as qualitative and quantitative qualities of the dispersed nanoparticles were studied using HRSEM coupled with EDX, model JEOL JSM-

7800F Field Emission Scanning Electron microscope (FESEM) coupled with Thermo Scientific Ultra dry EDS detector. Functional groups in the adsorbents were investigated using the PerkinElmer FTIR-ATR Spectrometer Frontier (Borken, Germany). Leaching studies of the loaded Fe into the hybrid resins was carried out to determine the loading capacity of each host material. About 0.5 g of each hybrid resin was shaken at 200 rpm with 10 mL 1 M HCl for 24 hours. This procedure was repeated 5 times with fresh leaching solution each time. All 5 aliquots were collected into a sample container for ICP-OES analysis, model Agilent Technologies 700 Series ICP-OES, USA.

### Equilibrium studies and isotherm modelling

Adsorption experiments were carried out using batch equilibrium technique, where about 50 mg/L single and binary Al and Mn solutions were prepared and used to model the adsorption of the synthesized adsorbents. The batch tests were carried out in 100 mL Erlenmeyer flasks using 50 mL of synthetic solution in an orbital shaker set at 200 rpm, at 25 °C. Each flask was covered with parafilm to avoid evaporation during the adsorption process. A fixed amount of adsorbent (e.g., 20 mg) was used for the kinetics study at different time intervals (5, 10, 20, 30, 60, 180, 360 minutes). Effect of adsorbent dosage (0–12 g/L) and initial pH (2–12) was also investigated. The amount of metal ions in the solutions was estimated using ICP-OES (Agilent Technologies 700 Series). All experiments were carried out in triplicate and the average result was reported. This was done to ensure accuracy, reliability and reproducibility of the collected data. Blanks were also run together with the samples to establish the effect the glassware has on the adsorption of the metal ions.

The amount of metal adsorbed per gram adsorbent, capacity  $q$  (mg/g), was calculated using Eq. 1:

$$q_e = \frac{V(C_o - C_e)}{m} \quad (1)$$

Where  $C_o$  and  $C_e$  are the initial and final concentration of the metal ion in solution (mg/L), respectively,  $V$  is the volume of solution used (L) and  $m$  is the mass of adsorbent (g)

### Kinetics studies

In this study three (3) kinetics models, mainly: pseudo-first-order, pseudo-second-order and intra-particle diffusion were applied to study the rates of adsorption which then informs about the adsorption mechanisms.

The pseudo-first-order (Lagergren) rate model postulates that physical interactions are responsible for the establishment

of an equilibrium between the liquid and the solid phase. This process is fully reversible and the linear form is given in Eq. 2:

$$\log(q_e - q_t) = \log q_e - \frac{K_{p1}}{2.303} t \quad (2)$$

Where  $q_e$  and  $q_t$  are the adsorbent capacity at equilibrium and at a particular time ( $t$ ), respectively.  $K_{p1}$  is the first order rate constant.

The pseudo-second-order (Langmuir) kinetics model assumes that the rate determining step involves chemical interactions leading to binding of metal ions on the adsorbent through strong covalent bonds. The linear form of this model is given in Eq. 3:

$$\frac{t}{q_t} = \frac{1}{K_{p2} q_e^2} + \frac{1}{q_e} t \quad (3)$$

If  $V_o$  is the initial adsorption rate, then  $V_o = K_{p2} q_e^2$  where  $K_{p2}$  is the second order rate constant.

The intra-particle diffusion model has been included to study the adsorption kinetics because the adsorbents under study are macroporous. This pore diffusion model best fits when the analyte particles are big and are in elevated concentrations in a well-mixed solution. The linear form of the intra-particle diffusion model used in this study is the Weber-Morris Model (Eq. 4):

$$q_t = K_{int} t^{\frac{1}{2}} \quad (4)$$

Where  $K_{int}$  is the intra-particle diffusion rate constant

### Isotherms

In this current study, two-parameter isotherm models namely: Freundlich, Langmuir and Temkin were employed to study the adsorption process of the metal ions on the hybrid Fe-oxide adsorbents.

The Freundlich model postulates that adsorption occurs on a heterogeneous surface where stronger binding sites are occupied first resulting to multiple layers of adsorbed material. The linear form of the Freundlich model is given in Eq. 5:

$$\log q_e = \log K_F + \left(\frac{1}{n}\right) \log C_e \quad (5)$$

Where  $K_F$  is the Freundlich constant which is related to the sorption capacity, that is, the higher the  $K_F$  value, the higher the sorption capacity of the solid material. The magnitude of  $n$  is a measure of favourability of adsorption by the adsorbent. When  $n = 1$  the adsorption is linear, when the adsorption is through chemisorption,  $n < 1$  and when it is through physisorption  $n > 1$ .

The Langmuir model claims that adsorption occurs on a homogeneous surface where all sites possess equivalent

binding energy. Once a site is occupied, no further sorption will take place resulting to a single layer of adsorbed material. The Langmuir model best describes the transfer of the analyte from the liquid phase (adsorbate) onto the surface of the solid (adsorbent). The linear equation of this model is given in Eq. 6:

$$\frac{C_e}{q_e} = \frac{C_e}{q_{max}} + \frac{1}{q_{max}K_L} \tag{6}$$

Where  $K_L$  is the Langmuir constant that reflects the affinity between the adsorbent and the adsorbate;  $q_{max}$  is the maximum adsorption capacity of the adsorbent.

The Temkin model is based on the assumption that the heat of adsorption decreases linearly with the increase of coverage of adsorbent due to adsorbate-adsorbate interactions. Therefore, it is widely used for the description of adsorption on heterogeneous surfaces. The linear form of the model is given in Eq. 7:

$$q_e = \frac{RT}{b} \ln k_T + \frac{RT}{b} \ln C_e \tag{7}$$

Where  $k_T$  is the Temkin constant

**Error function**

Error function assessment is used to evaluate the fit of an isotherm to the experimental results. The mostly used error function to predict the optimum kinetics or isotherm model for a particular set of results is the correlation coefficient,  $R^2$ . The best fit model is selected based on the magnitude of the coefficient of determination ( $R^2$ ). The model with coefficient of determination closest to 1 (unity) is considered the best fitting.

**Results and discussions**

**Characterization of resins**

**X-ray diffractometry**

Figure 1 depicts the XRD spectra for the studied HFO hybrids. The wide and small diffraction peaks with poor resolution in the XRD spectra showed that the hybrid HFO adsorbents are amorphous in nature, which is desirable for enhanced adsorption sites. The attractiveness of having amorphous adsorbents can be explained from the fact that adsorption is a surface phenomenon, therefore a good adsorbent must have as much surface area as possible. This can be realized with amorphous particles which are loose and small in size, hence provide greater surface area which translates to increased active sites for adsorption to occur. In addition, the XRD analysis showed that the main Fe-oxide form present in the hybrid materials was goethite (FeOOH). This result is justified because during

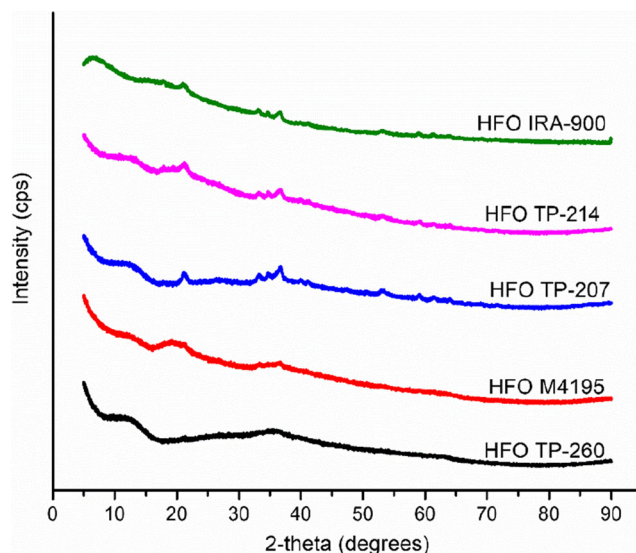
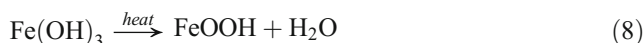


Fig. 1 X-ray diffraction spectra for the HFO hybrid adsorbents

the mild thermal treatment stage the produced ferric hydroxide loses a water molecule resulting into the goethite (Eq. 8).



**Fourier Transform Infrared**

The FTIR analysis results shown in Fig. 2 confirm the presence of goethite in all the adsorbents under study by the appearance of bands at about 671 and finger-like bands between 795 and 890  $\text{cm}^{-1}$  which are ascribed to the Fe-O vibration modes of the FeOOH [27]. Literature attests that O-H stretching give rise to a strong peak between 3000 and 3700

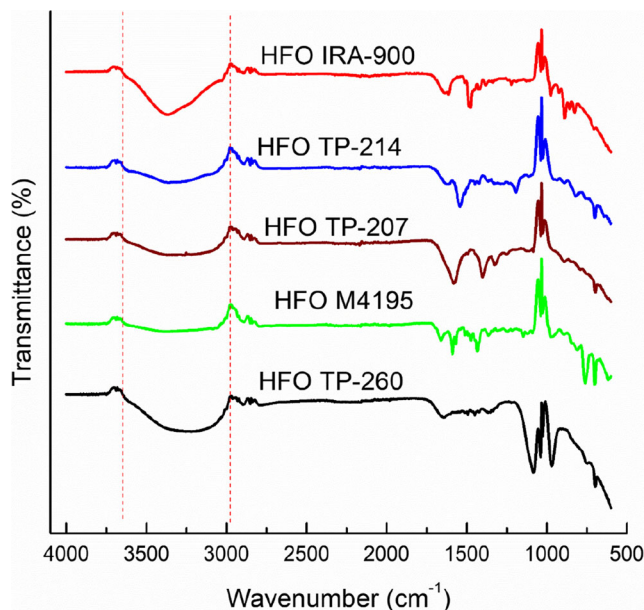


Fig. 2 FTIR spectra for the HFO hybrid adsorbents

$\text{cm}^{-1}$  [28] which is in agreement with the findings of Zheng et al. [29] who reported the O-H stretching bond at  $3367.1 \text{ cm}^{-1}$ . Therefore, the broad band at  $3250 \text{ cm}^{-1}$  confirms the presence of hydroxyl ions in all the HFO hybrids.

### Scanning Electron Microscopy

The HRSEM image of HFO TP-260 and its EDX showing the Fe loading in the organic/inorganic adsorbent is presented in Fig. 3. The SEM image shows that the Fe-oxide nanoparticles formed rods within the polymeric material. The EDX point spectrums show that there is even distribution of the Fe-oxide nanoparticles within the resin beads. The percentage Fe composition by weight of the HFO hybrid adsorbents determined by EDX was found to be TP-260 (36.53), M4195 (39.07), TP-207 (12.96), TP-214 (9.29) and IRA-900 (3.09).

The Fe oxide was incorporated in all the host resins in different degrees. The Fe level in the leachate of each synthesised hybrid adsorbents is given in Table 1.

### Effect of contact time

The optimum contact time for the adsorption of  $\text{Al}^{3+}$  from solution by the hybrid resins was determined by carrying out the adsorption process at different time intervals. The adsorption capacities of the various adsorbents for Al ions in single and binary element solution at different time intervals are

presented in Fig. 4a and b, respectively. It was observed that the adsorption capacities of all the hybrid adsorbents were much enhanced in the binary (Al and Mn) solution than in the single Al solution. Secondly, the adsorption capacities of the hybrid adsorbents showed some variation with time in the single element solution yet in the binary solution the adsorption capacity is generally the same for all the time intervals. This observation suggests that time was a factor of adsorption for the single element solution while it generally did not affect adsorption in the binary solution.

Mn (II) was used to represent co-existing ions because it is abundant in AMD alongside with iron but the iron could not be used because its oxide has been used as the adsorbent in this work. The HFO adsorbents favour Al ions adsorption in the presence of the competing Mn (II) ions. This is shown by that the adsorption capacities of all the adsorbents are higher in the binary solution than in the single Al solution at a given contact time. This fact was corroborated by the use of an equimolar binary solution of Al and Mn to compare the affinity of the adsorbents for the two analytes. All the adsorbents showed higher affinity for the Al ion regardless of that its level is half that of the Mn ion in the equimolar solution. The HFO IRA-900 showed the lowest capacity in the binary solution because the host resin for the HFO is a strong base ion exchanger; it has non-diffusible positive charges. Hence it experiences dominant Donnan co-ion exclusion effect [16, 30] resulting in the analyte missing contact with the adsorption sites.

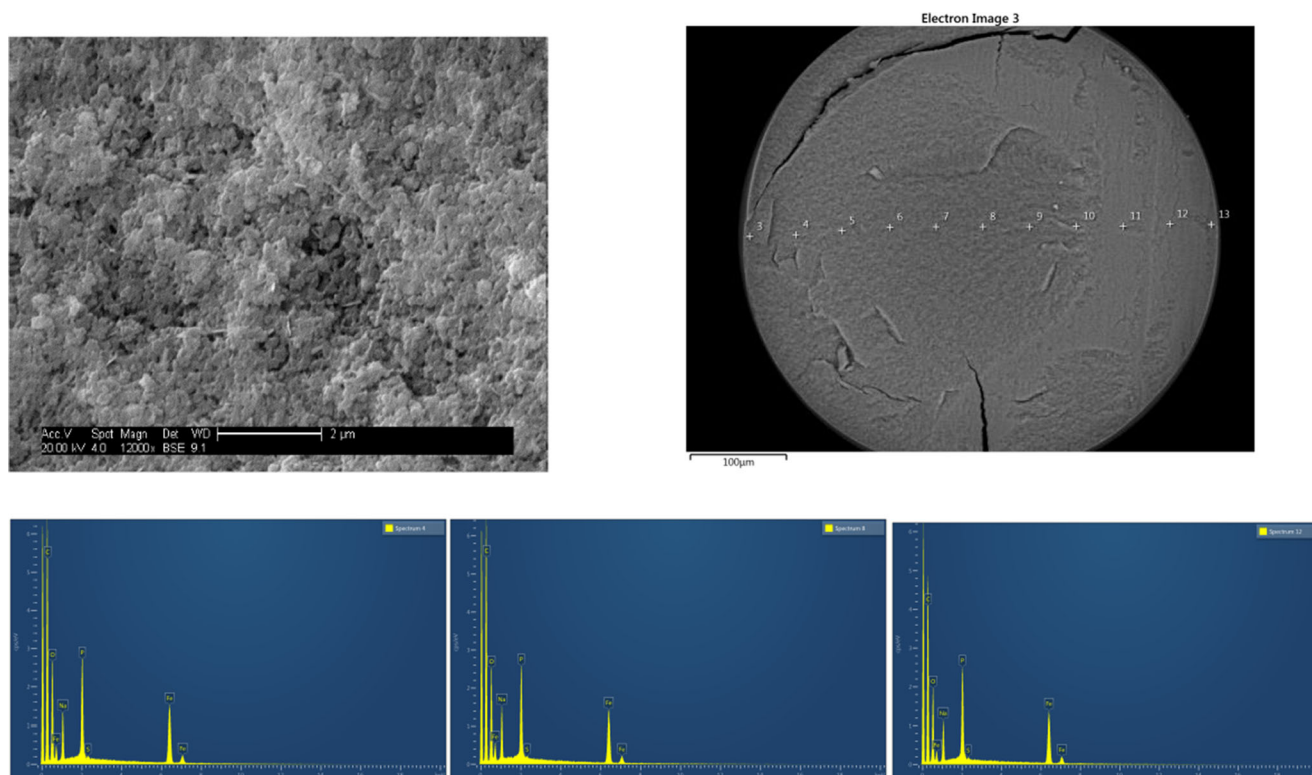


**Fig. 3** Scanning electron micrographs and EDX spectra for the HFO TP-260 bead cross-section

**Table 1** Mean loading capacities of HFO hybrid resins (mg Fe/g resin)

HFO hybrid resin	TP-260	TP-207	TP-214	M4195	IRA-900
Mean	42.1863	62.8437	6.8116	34.9048	11.1290
SD	1.2259	2.4508	0.3420	2.5029	0.9772

**Effect of resin dosage**

The effect of adsorbent dosage on the sorption of Al ions was studied using the 50 mg/L Al-Mn (II) binary solution at solution pH. Figure 5 shows that the amount of analyte adsorbed increases with increasing adsorbent dosage for hybrid TP-260 and TP-207 while with the other adsorbents more adsorbent dosage led to less Al adsorbed. This observation may be attributed to that hybrids TP-260 and TP-207 were the most loaded with the Fe-O moieties compared to their counterparts.

The host materials of these two hybrid materials were cation exchangers which, through the Donnan membrane effect, selectively pulled cationic species into the beads improving the adsorption on the dispersed abundant HFO particles. The contrary is true for hybrid M4195 and IRA-900 because their hosts were anionic exchangers. Therefore, the rejection of cationic species due to like charges with the fixed ones within

the anionic exchangers host resins led to the decrease in adsorption observed in Fig. 5. Hybrid TP-214 was acidic but followed the trend of the basic hosted hybrids. The anomalous behaviour may be attributed to that the hybrid had very little HFO loaded in it providing very few adsorption sites which get exhausted fast, not to the Donnan membrane effect.

**Effect of initial pH**

Solutions of about 50 mg/L Al (III) were adjusted to various initial pH values by addition of 1 M NaOH because the synthetic solution was very acidic (pH 1.7). Each hybrid resin was used for adsorption of Al ions from a binary solution with Mn (II) ions at its optimised contact time and dosage. Figure 6 shows the amount of Al (III) adsorbed by the various hybrid adsorbents at different initial solution pHs. Hybrid TP-260 and TP-207 removed all the Al ions from solution at acidic pH 2.41 and 3.16, respectively. Both hybrids can be used for remediation of Al from AMD but the later failed to produce a final solution that meet the international pH guideline (6.5 – 8.5) for drinking water set by United States Environmental Protection Agency (USEPA). The final solution pH was 6.81 for hybrid TP-260 and 5.87 for hybrid TP-207. Hybrid TP-214 and IRA-900 adsorbed all of the Al ions from solution in alkaline conditions (pH 9.73) but this may not be solely attributed to the effect of the adsorbents. Mn precipitates at about pH 9 forming hydrated Mn oxides which are renowned toxic metal adsorbents; Mn oxides are toxic metal scavengers in the environment. Therefore, the total removal of the Al ions may be attributed to a joint effort from both the adsorbent and the produced Mn precipitates. The results also show that in highly alkaline solution (pH 11) the adsorbed Al get desorbed which is implied by the sharp decrease of Al ions adsorbed. Finally, Fig. 6 shows that toxic metal adsorption is favourable in acidic pH while efficient desorption can be achieved in highly alkaline conditions. This may be attributed to that at higher pH the abundant O atoms of the hydroxide ions compete with those of the hydroxyl groups surrounding the metal ion in solution

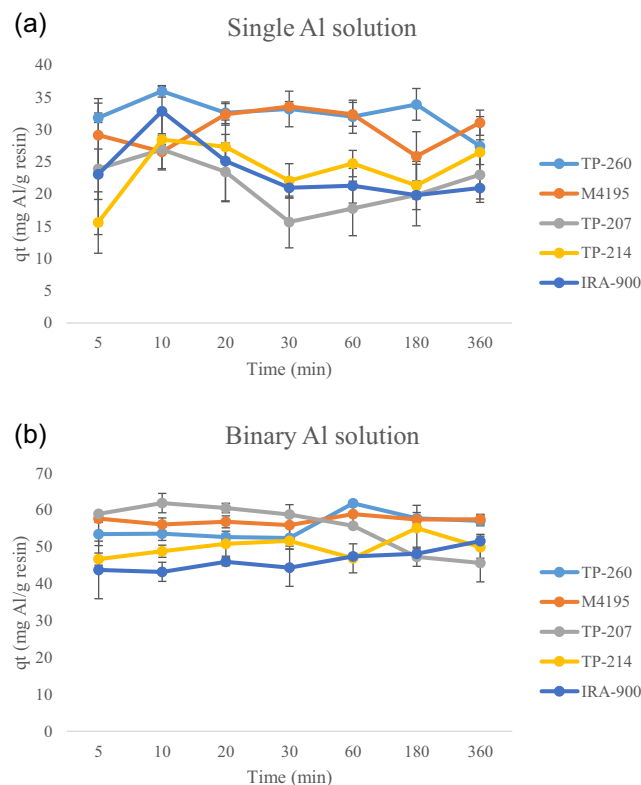


**Fig. 4** Kinetic studies on the adsorption of Al ions on the various adsorbents (50 mL synthetic solution containing 50 mg/L each of Al and Mn (II) ions; sorbent mass 20 mg; shaking speed 200 rpm; temperature 25 °C)

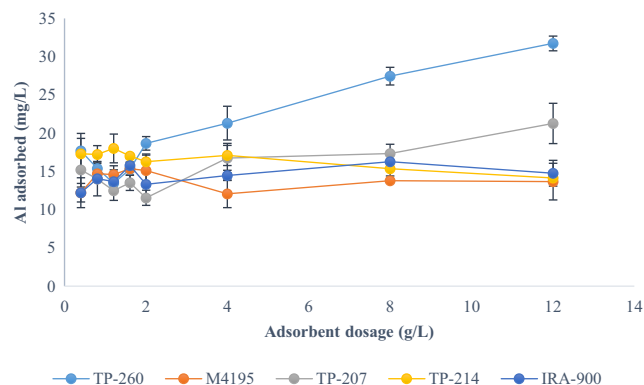


**Fig. 5** Effect of adsorbent amount on the sorption of Al<sup>3+</sup> by the hybrids (volume of sorption solution 50 mL containing 50 mg/L each of Al and Mn (II) ions; solution pH; shaking speed 200 rpm; temperature 25 °C)

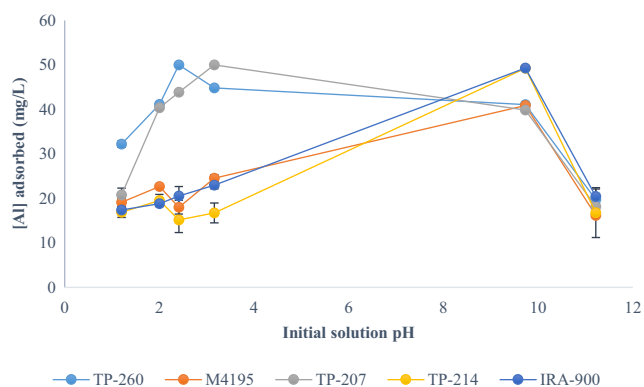


**Fig. 6** Effect of initial pH on the sorption of Al ions (50 mL synthetic solution of 50 mg/L each of Al and Mn (II) ions; stirring rate 200 rpm; temperature 25 °C)

for adsorption sites. The hydroxide ion O atoms are more reactive than those of the hydrated metal ion radius hence the less reactive was displaced from the adsorbent surface.

## Data modelling

### Kinetics

The efficiency of an adsorption process, which is the kinetics of adsorption, is determined by the rate at which metal ions are transferred from the liquid phase onto the surface of the adsorbent. The kinetic study enabled the researchers to gain insight into the adsorbent-adsorbate reaction pathways. Kinetics of best fit is the pseudo-second-order model. This is shown in Table 2 by the correlation coefficient closest to unity than the other two models. From this result it may be concluded that the Al(III) ions' adsorption onto the hybrid HFO adsorbents is of the pseudo-second order in nature. This result was confirmed in Table 3 which shows that the adsorbent

capacity calculated using the pseudo-second order kinetics is in agreement with the experimental one as compared to that of the pseudo-first-order kinetics model.

Al<sup>a</sup> –single Al solution, Al<sup>b</sup> – binary Al solution

### Isotherms

An isotherm is the equilibrium relationship between the analyte concentration in solution and that on the adsorbent surface at a given condition. It is a thermodynamic basic of separation processes and determines the extent at which the analyte can be adsorbed onto a particular surface [31]. Adsorption of Al ions by hybrid TP-260 followed the Freundlich model as shown by the coefficient of determination closest to unity (1) compared to the other investigated models for both single and binary elements solutions (Table 4). The value of  $n$  for the binary solution is greater than 1 which suggests that the adsorption on this hybrid was through formation of weak bonds forming multiple layers of adsorbate on the adsorbent. With the single element solution the adsorption was through formation of strong bonds (chemisorption) as concluded from the value of  $n$  that is less than 1. The value of  $K_F$  is directly proportional to sorption capacity. Thus, from the higher values of  $K_F$  for the single element solution than for the binary solution, it can be concluded that the sorption capacity of the hybrid resin was higher when there was no competition of adsorption sites from the coexisting Mn(II) ions.

Adsorption by hybrid M4195 in the binary solution followed the Temkin model which suggests that as the adsorption was progressing the energy of the adsorption sites was decreasing. In the single element solution the hybrid best fitted the Freundlich model through physisorption with high sorption capacity. Hybrid TP-207 exhibited high adsorption capacity for Al(III) in the binary solution through physisorption as

**Table 2** Parameters of adsorption kinetics models for Al<sup>3+</sup> on hybrid HFO nanocomposites

Resin HFO	Analyte	Pseudo-second-order		Pseudo-first-order		Intra-particle	
		$K_{2p}$	$R^2$	$K_{1p}$	$R^2$	$K_{int}$	$R^2$
Aluminium							
TP-260	Al <sup>b</sup>	0.0917	0.9997	0.0032	0.1230	0.2958	0.2717
	Al <sup>a</sup>	-0.0057	0.9916	-0.0009	0.0097	-0.2798	0.4334
M4195	Al <sup>b</sup>	0.6055	1.0000	0.0037	0.1220	0.0513	0.0923
	Al <sup>a</sup>	0.0192	0.9903	0.0012	0.0118	-0.0305	0.0038
TP-207	Al <sup>b</sup>	-0.0040	0.9993	-0.0044	0.1537	-1.0182	0.9232
	Al <sup>a</sup>	0.0060	0.9922	0.0005	0.0033	-0.1053	0.0272
TP-214	Al <sup>b</sup>	-0.0335	0.9975	0.0035	0.1504	0.2006	0.1759
	Al <sup>a</sup>	$7.5 \times 10^{-7}$	0.9871	0.0021	0.0526	0.1453	0.0402
IRA-900	Al <sup>b</sup>	0.0050	0.9989	0.0069	0.6259	0.4588	0.9045
	Al <sup>a</sup>	-0.0432	0.9990	-0.0014	0.0290	-0.3987	0.2940



**Table 3** Comparison of experimental and calculated capacity (mg/g) using kinetic models

HFO hybrid		TP-260	M4195	TP-207	TP-214	IRA-900
Experimental		61.8475	58.9440	61.9286	55.1438	51.6229
Calculated	1 <sup>st</sup> - order	9.34545	3.6283	3.9747	8.0575	10.8693
	2 <sup>nd</sup> - order	57.4713	57.4713	45.2489	50.7614	51.5464

concluded from that the high Freundlich constant,  $K_F$ . In the single element solution Al(III) adsorption followed the Langmuir model. It is noteworthy that the negative value of the Langmuir constant indicate that the model is inadequate to describe the adsorption process regardless of that it gave the highest correlation of determination [32, 33]. Hybrid TP-214 and IRA-900 adsorbed Al in single layer regardless of existence of competition from other ions, both hybrids fitted into the Langmuir model although the model cannot describe the adsorption process adequately due to the negative  $K_L$  values as mentioned earlier.

Al<sup>a</sup> - single ion solution, Al<sup>b</sup> - binary solution

**Application of hybrid adsorbent in the treatments of environmental AMD**

The hybrid HFO resins were used to adsorb toxic metals (Al, Cd, Co, Cr, Cu, Fe, Mn, Ni, Pb, Zn) from AMD (pH 2.57) sampled from a defunct gold mine old shaft in the western part of Johannesburg. The hybrid adsorbents were used in their respective optimised conditions which were predetermined by the batch adsorption studies. Figure 7 shows the levels of the various toxic metals in the untreated AMD and the amount adsorbed by the various synthesized hybrid ion exchange iron oxide nanocomposites. All the selected toxic metals were detected in the sampled acidic water. The adsorption affinity of hybrid TP-260 superseded all the other adsorbents in all the toxic metals removed except for Cu and Co which were best adsorbed by hybrid M4195 and TP-207, respectively. The

observation on superior Cu adsorption by hybrid M4195 is not surprising because it is in agreement with what is reported by Edebali and Pehlivan [34]. They found that Cu (II) ions have high affinity for Dowex M4195 which is the host resin for this hybrid HFO adsorbent. Karimpour and others reported high removal efficiency for Cd and Pb ions at neutral pH (7) and enhanced temperature (35 °C) by dead bacteria cells [35] whereas, hybrid TP-260 removed metals from a complex solution (AMD) in very acidic conditions (pH 2.57) at ambient temperature (25 °C). The metal removal efficiency of the dead bacteria adsorbent decreased with decreasing solution pH. This is in agreement with findings by Karapmar (2016) who conducted an investigation on the use of ferrihydrite (Fe(III) precipitate) for the removal of heavy metal ions from solutions of different pH. They found that the removal of Pb(II), Cu(II) and Zn(II) was lower at low pH conditions typical of AMD [36]. Therefore, hybrid TP-260 showed superior performance in removal of metals from hostile conditions which other adsorbents cannot withstand.

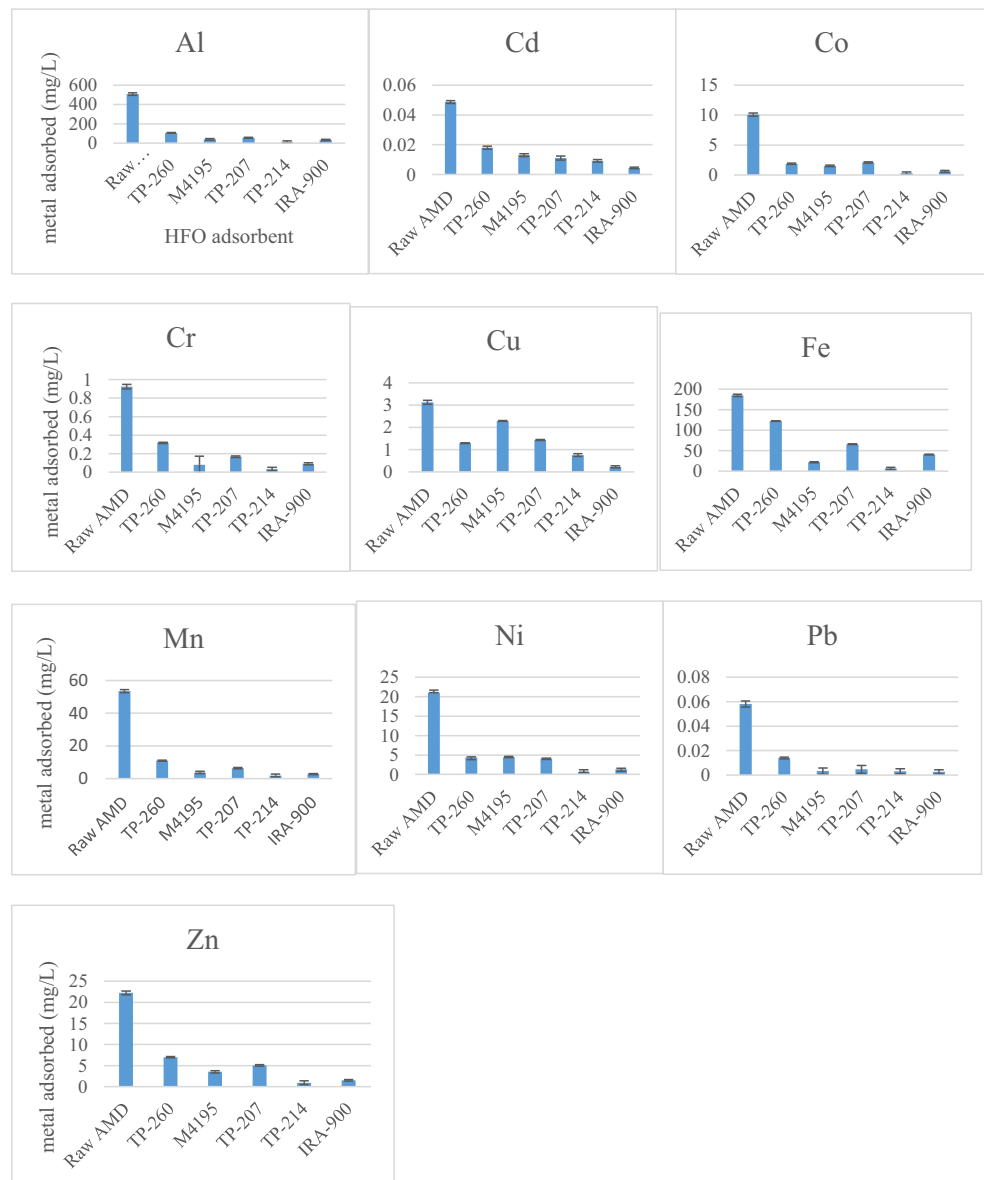
**Regeneration studies**

The hybrid TP-260 was evaluated for re-usability by using regenerant solutions of different pH to desorb Al(III) from the loaded resins. The regenerant solutions that were used are NaCl-NaOH (pH 12.5), NaCl-NH<sub>2</sub>OH.HCl (pH 3.0) and NaCl-HCl (pH 3.2) binary solutions. Figure 8 shows that Al(III) can be desorbed efficiently in highly alkaline conditions which is expected because the adsorption was

**Table 4** Parameters of adsorption isotherm models for Al<sup>3+</sup> on hybrid HFO nanocomposites

Resin HFO	Analyte	Freundlich			Langmuir		Temkin		
		$K_F$	n	R <sup>2</sup>	$K_L$	R <sup>2</sup>	$K_T$	R <sup>2</sup>	
Aluminium	TP-260	Al <sup>b</sup>	0.0042	2.184	0.9511	-0.0197	0.9031	0.0619	0.8881
		Al <sup>a</sup>	39.5367	-1.6276	0.5293	-0.3237	0.4635	0.0111	0.4458
M4195	TP-207	Al <sup>b</sup>	1.51x10 <sup>-20</sup>	13.498	0.8437	-0.0254	0.6940	0.0299	0.9274
		Al <sup>a</sup>	7.35x10 <sup>26</sup>	-0.0583	0.7917	-0.0305	0.7320	0.0265	0.6757
TP-214	IRA-900	Al <sup>b</sup>	5.43x10 <sup>28</sup>	-17.655	0.8534	-0.0292	0.8480	0.02582	0.7716
		Al <sup>a</sup>	1.3709	-51.546	0.0827	-1.3268	0.9940	2.37x10 <sup>-25</sup>	0.0719
IRA-900	Al <sup>b</sup>	Al <sup>b</sup>	1.61x10 <sup>49</sup>	-31.65	0.7313	-0.0306	0.9132	0.0282	0.3765
		Al <sup>a</sup>	7.50x10 <sup>26</sup>	-0.0575	0.8334	-0.0302	0.8774	0.0266	0.6801
IRA-900	Al <sup>b</sup>	Al <sup>b</sup>	3.59x10 <sup>-35</sup>	22.706	0.7289	-0.0265	0.7959	0.0293	0.5755
		Al <sup>a</sup>	8.95x10 <sup>8</sup>	-0.1707	0.3293	-0.0304	0.4541	0.0214	0.2543

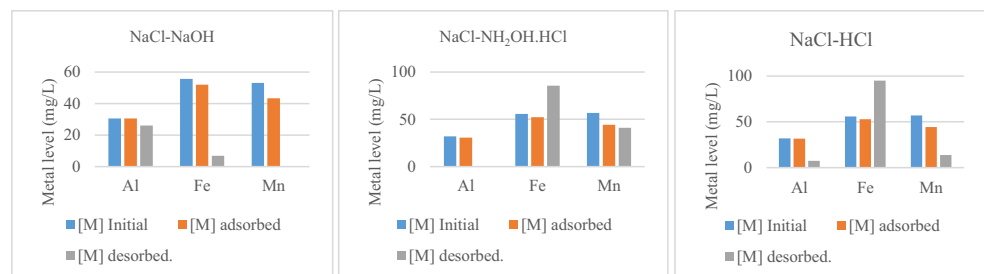
**Fig. 7** Toxic metal amount (mg/L) adsorbed by the respective hybrid sorbents and metal level in the AMD before treatment



unfavourable at about pH 11 (Fig. 6). The co-existing Fe(II) and Mn(II) could not be desorbed in alkaline conditions but in acidic conditions. The higher Fe levels in the regenerant effluent observed when using strongly acidic regenerants may be attributed to the leaching of the embedded HFO which leads to the destruction of the hybrid adsorbent, hence NaCl-

NH<sub>2</sub>OH.HCl and NaCl-HCl are not suitable regenerants for HFO adsorbents. It can be inferred that the Fe and Mn are adsorbed on different sites of the adsorbent from those on which Al is adsorbed. It may be recommended that the metal loaded hybrid resins should be regenerated using more than one solutions in series. The different solutions will regenerate

**Fig. 8** Regeneration of hybrid TP-260 using different regeneration binary solutions



different kinds of adsorption sites in the hybrid adsorbent. Therefore, further studies on the investigation of suitable desorbents and regeneration cycles need to be undertaken.

## Conclusions and Recommendations

A variety of hybrid iron oxide nanocomposites using macroporous chelating resins with different functional groups as the host materials for HFO nanoparticles were successfully synthesized using the in-situ precipitation method followed by mild thermal treatment. Hybrid TP-260 removed all the Al ions from the binary solution with Mn at pH 2.41 concomitantly raising the pH of the solution to 6.81 which is within the set standard by USEPA for drinking water. At pH higher than 10, the adsorbed Al got desorbed which indicates that desorption of the loaded hybrid adsorbent can be efficiently carried out at this pH range. It may be concluded that the solution pH plays a crucial role in the adsorption/desorption of toxic metals on hybrid iron oxide adsorbents. Toxic metal sorption is more effective in binary/multi component solutions than in single component solutions which is advantageous for purpose. This advantage of HLIX adsorbents was manifested on the adsorption of ten (10) toxic metal ions from AMD, where all the metals analysed were adsorbed in different degrees by all the adsorbents. Hybrid TP-260 is the best choice because it has higher adsorption capacity for most of the toxic metals investigated in this study.

## References

- Mulopo J. Continuous pilot scale assessment of the alkaline barium calcium desalination process for acid mine drainage treatment. *J Environ Chem Eng.* 2015;3:1295–302. <https://doi.org/10.1016/j.jece.2014.12.001>.
- Feng D, Aldrich C, Tan H. Treatment of acid mine water by use of heavy metal precipitation and ion exchange. *Miner Eng.* 2000;13:623–42. [https://doi.org/10.1016/S0892-6875\(00\)00045-5](https://doi.org/10.1016/S0892-6875(00)00045-5).
- Durand JF. The impact of gold mining on the Witwatersrand on the rivers and karst system of Gauteng and North West Province, South Africa. *J Afr Earth Sci.* 2012;68:24–43. <https://doi.org/10.1016/j.jafrearsci.2012.03.013>.
- Park JH, Edraki M, Mulligan D, Jang HS. The application of coal combustion by-products in mine site rehabilitation. *J Clean Prod.* 2014;84:761–72. <https://doi.org/10.1016/j.jclepro.2014.01.049>.
- Akcil, Koldas S. Acid Mine Drainage (AMD): causes, treatment and case studies. *J Clean Prod.* 2006;14:1139–45. <https://doi.org/10.1016/j.jclepro.2004.09.006>.
- Planning, W. Q. *Treatment Technology Options*; 2013; ISBN 9780621414172.
- Fu F, Wang Q. Removal of heavy metal ions from wastewaters: A review. *J Environ Manag.* 2011;92:407–18. <https://doi.org/10.1016/j.jenvman.2010.11.011>.
- Padunthong S, German M, Wiriyathamcharoen S, SenGupta AK. Polymeric anion exchanger supported hydrated Zr(IV) oxide nanoparticles: A reusable hybrid sorbent for selective trace arsenic removal. *React Funct Polym.* 2015;93:84–94. <https://doi.org/10.1016/j.reactfunctpolym.2015.06.002>.
- Samiey B, Cheng C, Wu J. Organic-Inorganic Hybrid Polymers as Adsorbents for Removal of Heavy Metal Ions from Solutions: A Review. *Materials (Basel).* 2014;7:673–726. <https://doi.org/10.3390/ma7020673>.
- Acelas NY, Martin BD, López D, Jefferson B. Selective removal of phosphate from wastewater using hydrated metal oxides dispersed within anionic exchange media. *Chemosphere.* 2015;119:1353–60. <https://doi.org/10.1016/j.chemosphere.2014.02.024>.
- Xu P, Ming G, Lian D, Ling C, Hu S, Hua M. Use of iron oxide nanomaterials in wastewater treatment : A review. *Sci Total Environ.* 2012;424:1–10. <https://doi.org/10.1016/j.scitotenv.2012.02.023>.
- Sarkar S, Chatterjee PK, Cumbal LH, SenGupta AK. Hybrid ion exchanger supported nanocomposites: Sorption and sensing for environmental applications. *Chem Eng J.* 2011;166:923–31. <https://doi.org/10.1016/j.cej.2010.11.075>.
- Sylvester P, Westerhoff P, Möller T, Badruzzaman M, Boyd O. A Hybrid Sorbent Utilizing Nanoparticles of Hydrated Iron Oxide for Arsenic Removal from Drinking Water. *Environ Eng Sci.* 2007;24:104–12. <https://doi.org/10.1089/ees.2007.24.104>.
- Puttamraju P, SenGupta AK. Evidence of tunable on-off sorption behaviors of metal oxide nanoparticles: Role of ion exchanger support. *Ind Eng Chem Res.* 2006;45:7737–42. <https://doi.org/10.1021/ie060803g>.
- Pan B, Wu J, Pan B, Lv L, Zhang W, Xiao L, et al. Development of polymer-based nanosized hydrated ferric oxides (HFOs) for enhanced phosphate removal from waste effluents. *Water Res.* 2009;43:4421–9. <https://doi.org/10.1016/j.watres.2009.06.055>.
- Cumbal L, Sengupta AK. Arsenic removal using polymer-supported hydrated iron ( III ) oxide nanoparticles : Role of Donnan Membrane Effect †. 2005, 39, 6508–6515.
- Nassar NN. Iron Oxide Nanoadsorbents for removal of various pollutants from wastewater: An overview. *Appl Adsorbents Water Pollut Control.* 2012;81–118.
- Klimkova S, Cernik M, Lacinova L, Filip J, Jancik D, Zboril R. Zero-valent iron nanoparticles in treatment of acid mine water from in situ uranium leaching. *Chemosphere.* 2011;82:1178–84. <https://doi.org/10.1016/j.chemosphere.2010.11.075>.
- Cumbal L, Greenleaf J, Leun D, SenGupta AK. Polymer supported inorganic nanoparticles: Characterization and environmental applications. *React Funct Polym.* 2003;54:167–80. [https://doi.org/10.1016/S1381-5148\(02\)00192-X](https://doi.org/10.1016/S1381-5148(02)00192-X).
- Sarkar S, Guibal E, Quignard F, SenGupta AK. Polymer-supported metals and metal oxide nanoparticles: Synthesis, characterization, and applications. *J Nanopart Res.* 2012;14. <https://doi.org/10.1007/s11051-011-0715-2>.
- Beker U, Cumbal L, Duranoglu D, Kucuk I, Sengupta AK. Preparation of Fe oxide nanoparticles for environmental applications: Arsenic removal. *Environ Geochem Health.* 2010;32:291–6. <https://doi.org/10.1007/s10653-010-9301-2>.
- SenGupta A. Hybrid anion exchanger for selective removal of contaminating ligands from fluids and method of manufacture thereof 2007. p. 2.
- Doula MK. Simultaneous removal of Cu, Mn and Zn from drinking water with the use of clinoptilolite and its Fe-modified form. *Water Res.* 2009;43:3659–72. <https://doi.org/10.1016/j.watres.2009.05.037>.
- Wang CC, Chen CY, Chang CY. Synthesis of chelating resins with iminodiacetic acid and its wastewater treatment application. *J Appl Polym Sci.* 2002;84:1353–62. <https://doi.org/10.1002/app.10243>.
- Donia AM, Atia AA, El-Boraey HA, Mabrouk DH. Adsorption of Ag(I) on glycidyl methacrylate/N,N'-methylene bis-acrylamide

- chelating resins with embedded iron oxide. *Sep Purif Technol.* 2006;48:281–7. <https://doi.org/10.1016/j.seppur.2005.07.034>.
26. Donia AM, Atia AA, Elwakeel KZ. Recovery of gold(III) and silver(I) on a chemically modified chitosan with magnetic properties. *Hydrometallurgy.* 2007;87:197–206. <https://doi.org/10.1016/j.hydromet.2007.03.007>.
  27. Kuang L, Liu Y, Fu D, Zhao Y. *Journal of Colloid and Interface Science* FeOOH-graphene oxide nanocomposites for fluoride removal from water : Acetate mediated nano FeOOH growth and adsorption mechanism. *J Colloid Interface Sci.* 2017;490:259–69. <https://doi.org/10.1016/j.jcis.2016.11.071>.
  28. Huang Y, Hsueh C, Huang C, Su L, Chen C. Adsorption thermodynamic and kinetic studies of Pb ( II ) removal from water onto a versatile Al<sub>2</sub>O<sub>3</sub> -supported iron oxide. 2007;55:23–9. <https://doi.org/10.1016/j.seppur.2006.10.023>.
  29. Zheng H, Gao X, Song L, Guo H. Preconcentration of trace aluminum ( III ) ion using a nanometer-sized TiO<sub>2</sub> -silica composite modified with 4-aminophenylarsonic acid , and its determination by ICP-OES. *Microchim Acta.* 2011;175:225–31. <https://doi.org/10.1007/s00604-011-0667-3>.
  30. Alonso A, Macanás J, Davies GL, Gun YK. Nanocomposites with most favorable distribution of catalytically active and biocide nanoparticles. 2010.
  31. Dubey S, Banerjee S, Nath S, Chandra Y. Application of common nano-materials for removal of selected metallic species from water and wastewaters : A critical review. *J Mol Liq.* 2017;240:656–77. <https://doi.org/10.1016/j.molliq.2017.05.107>.
  32. Alsenani G. Studies on adsorption of crystal violet dye from aqueous solution onto calligonum comosum leaf powder (CCLP). *J Am Sci.* 2013;9:30–5.
  33. Alshabanat M, Alsenani G, Almufarj R. Removal of crystal violet dye from aqueous solutions onto date palm fiber by adsorption technique. *J Chem.* 2013;2013:1–6. <https://doi.org/10.1155/2013/210239>.
  34. Edeballi S, Pehlivan E. Evaluation of chelate and cation exchange resins to remove copper ions. *Powder Technol.* 2016;301:520–5. <https://doi.org/10.1016/j.powtec.2016.06.011>.
  35. Karimpour M, Davoud S. Data in brief adsorption of cadmium and lead onto live and dead cell mass of *Pseudomonas aeruginosa* : A dataset. *Data Br.* 2018;18:1185–92. <https://doi.org/10.1016/j.dib.2018.04.014>.
  36. Karap N, Removal of heavy metal ions by ferrihydrite : an opportunity to the treatment of acid mine drainage. 2016, <https://doi.org/10.1007/s11270-016-2899-7>.

**Publisher's note** Springer Nature remains neutral with regard to jurisdictional claims in published maps and institutional affiliations.